TECHNICAL TRANSACTIONS | CZASOPISMO TECHNICZNE
MECHANICS | MECHANIKA
1-M/2016

PAVEL DITL, RADEK ŠULC*

DISPERSION KINETICS MODELLING

MODELOWANIE KINETYKI DYSPERGOWANIA

Abstract

Stirred tanks for dispersion, the pre-dispersion of two immiscible liquids or particulate solid-liquid suspension are extensively used in the chemical, food, pharmaceutical and metallurgical industries, for purposes such as suspension/emulsion polymerisation, heterogeneous/phase-transfer catalytic chemical reactions, paint production and hydrometallurgical solvent extraction. The aim of this paper is to propose the simple dispersion model enabling the prediction of particle size changes over time and taking into account the type of breakup mechanisms, the non-homogeneity of local turbulent energy dissipation rate in an agitated vessel and the effect of the number of times the liquid passes through the impeller and the impeller zone. The model was successfully tested on data published by Ditl et al. (1981).

Keywords: *dispersion kinetics modelling, solid particle-liquid dispersion, tooth impeller*

Streszczenie

Mieszalniki do sporządzania mieszanin lub dyspergowania płynów niemieszających się są szeroko stosowane w przemyśle chemicznym, spożywczym, farmaceutycznym, metalurgicznym i wielu innych gałęziach przemysłu. Celem pracy jest przedstawienie prostego modelu dyspersji umożliwiający prognozowanie zmian wielkości cząstek w czasie z uwzględnieniem różnych mechanizmów rozpadu, niejednorodności lokalnych burzliwych szybkości rozpraszania energii w mieszalniku oraz liczby przejść płynu przez obszar mieszadła. Model ten został z powodzeniem przetestowany na danych opublikowanych przez Ditl et al. (1981).

Słowa kluczowe: *modelowanie kinetyki dyspersji, układ dyspersyjny cząstki ciała stałego-płyn, mieszadło ścinające*

DOI:

* Prof. PhD. DSc. Eng. Pavel Ditl, Assoc. prof. PhD. DSc. Eng. Radek Šulc, Department of Process Engineering, Faculty of Mechanical Engineering, Czech Technical University in Prague.

1. Introduction

Stirred tanks for dispersion, the pre-dispersion of two immiscible liquids or particulate solid-liquid suspension are extensively used in the chemical, food, pharmaceutical and metallurgical industries, for purposes such as suspension/emulsion polymerisation, heterogeneous/phase-transfer catalytic chemical reactions, paint production and hydrometallurgical solvent extraction [1-3]. Mixing plays a fundamental role in these systems controlling processes such as blending, homogenisation, mass transfer and chemical reactions etc. The quality of product, yield and economy of the processes is therefore significantly affected by mixing. Insufficient or excessive mixing may lead to wastage of processing time and raw material and/or the formation of by-products [4, 5].

The prediction of mean drop/particle size and drop/particle size distribution (DSD) is vital for emulsification, suspension polymerisation, solid particle dispersion or crystallisation. Important process variables such as particle/drop size and size distribution are strongly affected by turbulence kinetic energy dissipation rate ε and its distribution in an agitated vessel.

2. Theoretical background

2.1. Liquid-liquid dispersion

If acting mechanical forces are greater than drop interface surface forces, the drops deform and split into two or more smaller drops. Since this process is random, different sizes of daughter drops are produced. After a period of time, the equilibrium drop size distribution that is independent of the previous history is reached. Two possible mechanisms of dispersion are usually considered: drop break up by viscous forces and drop break up by inertial forces. The drop breakup mechanism is controlled by the turbulent eddy size [6].

If the breakup occurs in the viscous subrange, i.e. $d_p < \eta_K$, the drop breakup is controlled by viscous forces, hence the drop size d_p can be expressed as follows [7]:

$$d_p \propto \frac{\sigma}{(\rho_c \cdot \mu_c \cdot \varepsilon)^{1/2}}, \tag{1}$$

where

ε – the local turbulent energy dissipation rate;
η_K – the Kolmogorov length microscale;
ρ_c, σ, μ_c – the physical properties of continuous fluid, i.e. density, interfacial tension, dynamic viscosity respectively.

If the breakup occurs in the inertial subrange, i.e. $\Lambda > d_p > \eta_K$, drop breakup is controlled by inertial forces, hence the drop size d_p can be expressed as follows [8]:

$$d_p \propto \sigma^{3/5} \cdot \rho_c^{-3/5} \cdot \varepsilon^{-2/5}, \tag{2}$$

To characterise equilibrium drop distribution, many authors used Sauter mean diameter d_{32}. Assuming that $\varepsilon \propto N^3 \cdot d^2$, Equation (2) is rewritten into a dimensionless form as follows:

$$d_{32}/d \propto We^{-3/5} , \tag{3}$$

where

d – the impeller diameter;.
We – the Weber number; $We = \rho_c \cdot N^2 \cdot d^3/\sigma$.

The mentioned correlations are only valid for dilute dispersions with a non-viscous dispersed phase where the viscous energy within the drops is negligible compared to its surface energy and the coalescence phenomenon is negligible. However, in the concentrated coalescing dispersions, the drop size is affected by both the breakup and the coalescence processes. It is assumed that the breakup occurs in the impeller region whilst the coalescence occurs mainly in the bulk region (e.g. [9]). Moreover, the dispersed-phase viscous forces contribute to the drop stability when $\mu_d > \mu_c$.

Many correlations describing the dependence of the Sauter diameter on the physical properties of fluids take both of the influences above mentioned into account by the relation in the following general form:

$$d_{32}/d \propto \left[1 + f_1(\varphi)\right] \cdot \left[1 + f_2(Vi)\right] \cdot We^{-n} , \tag{4}$$

where

φ – the dispersed-phase volume fraction in the system;
Vi – the viscosity group, $Vi = \mu_d/(d \cdot \rho_d \cdot \sigma)^{1/2}$;
n – the Weber number´s exponent.

In the breakup region the Weber number´s exponent is 0.6 [8]. In the coalescence region the exponent n is 3/8 [10]. Many authors use the Weber number´s exponent as an adjustable parameter. For example, Desnoyer et al. [11] take into account the effect of the dispersed-phase volume fraction φ on d_{32} considering the effect of the dispersed-phase fraction on the Weber number exponent n and on the constants of proportionality. According to Bałdyga and Podgórska [12], drop size depends on the fine-scale intermittency when the turbulence has intermittent character. In this case, the value of the Weber exponent depends on a intermittency scaling exponent.

The published correlations for d_{32} assume steady state. The time to reach the equilibrium drop size distribution depends on the number of times the liquid passes through the impeller zone and the bulk zone. Following this fact the number of passages through these spaces is crucial for dispersion kinetics modelling as confirmed by Šulc and Ditl [13] for flocculation kinetics modelling.

Currently, the most common approach to predicting drop size distribution and its time evolution in agitated vessels is based on population balance models (e.g. [14, 15]).

However, the quality of the prediction strongly depends on the quality of used breakage and coalescence kernels and the estimation of the local turbulent energy dissipation rate.

2.2. Solid particle-liquid dispersion

Compared with liquid-liquid dispersion, the mechanisms of solid particle-liquid dispersion is less complicated due to the rigid character of solid particles, especially when broken particles do not re-aggregate. In this case, only the breakup process occurs.

The aim of this paper is to propose a simple model of dispersion kinetics for the prediction of the time course of solid particle size taking into account the type of breakup mechanisms, the non-homogeneity of the local turbulent energy dissipation rate in an agitated vessel and the effect of the number of times the liquid passes through the impeller. The model was successfully tested on data published by Ditl et al. [16].

3. Kinetics model

For particle breaking occurring in a mechanically agitated vessel in the inertial subrange, i.e. $\Lambda > d_p > \eta_K$, the following assumptions were postulated: 1) the breaking occurs during passage through the impeller only; 2) broken particles do not re-aggregate; 3) the minimum particle size is limited by the Kolmogorov length microscale η_K corresponding to the mixing intensity in the impeller zone; 4) the change of particle size can be described by first-order kinetics as follows:

$$-\frac{\mathrm{d}(d_p)}{\mathrm{d}t} = k \cdot (d_p - d_{pf}) , \tag{5}$$

where

k – the breaking rate-constant;
d_p – actual particle size in time t;
d_{pf} – the final particle size.

Integrating Equation (5) for the initial condition d_p (t = 0) = d_{p0} the time dependency of particle size d_p can be obtained as follows:

$$\frac{d_p - d_{pf}}{d_{p0} - d_{pf}} = \exp(-k \cdot t) , \tag{6}$$

where

d_{p0} – the initial particle size.

Taking the number of passages of liquid through an impeller into account, Equation (6) can be rewritten as follows:

$$d_p^* = \frac{d_p - d_{pf}}{d_{p0} - d_{pf}} = \exp(-k^* \cdot N \cdot t)\,, \tag{7}$$

where

k^* – the dimensionless breaking rate-constant;
d_p^* – dimensionless particle size;
N – the impeller rotational speed.

The Kolmogorov length microscale η_K is defined as follows:

$$\eta_K = \left(\frac{\nu^3}{\varepsilon}\right)^{1/4}, \tag{8}$$

where

ν – the kinematic viscosity of agitated liquid;
ε – the turbulent energy dissipation rate.

The turbulent energy dissipation rate in the impeller zone was estimated from impeller power input using swept volume approach and assuming that the practically whole impeller power is dissipated in the impeller zone. Thus, the final particle size was estimated as follows:

$$d_{pf} \approx (\eta_K)_{imp} = \left(\frac{\nu^3}{(P/m)_{imp}}\right)^{1/4} = \left(\frac{\nu^3}{(P/(\rho \cdot V_{imp})}\right)^{1/4}, \tag{9}$$

where

P – the impeller power input;
$(P/m)_{imp}$ – the specific turbulent energy dissipation rate in the impeller zone;
V_{imp} – the volume occupied by the rotating impeller.

4. Data analysis

The proposed model was tested on data published by Ditl et al. [16]. Ditl et al. [16] studied the time course of the dispersion of TiO_2 particles in liquid. The effect of impeller rotational speed, impeller type, vessel shape, impeller diameter to vessel diameter ratio, and solid particle concentration on dispersion was investigated. The effect of impeller rotational speed was investigated in a square vessel measuring 0.15 m × 0.15 m agitated by a tooth impeller having D/d = 4.54. The authors' attention was also focused on the scale-up of dispersion. On the basis of results derived for the disc impeller by Schlichting [17], the authors proposed scale-up rule $N \cdot d^{0.89}$ = const. using which the turbulent shear strength on tooth impeller surface should be maintained constant. The scaling experiments were carried out in cylindrical vessels of various vessel diameters D agitated by a tooth impeller having D/d = 3.

The mentioned experimental results were used in this work for the testing of the proposed model. In accordance with the model assumptions, particle sizes measuring less than the estimated Kolmogorov length microscale were not taken into account. The evaluated model parameters are presented in Table 1. The comparison of experimental and predicted dependence of particle size on time is presented in Fig. 1 for data measured in the squared vessel and in Fig. 3 for data measured in the cylindrical vessel. The comparison of experimental data and the time course predicted by the model are presented in dimensionless form for the squared and cylindrical vessel in Fig. 2 and Fig. 5, respectively. The effect of dimensionless time $N.t$ taking the number of times the liquid passes through the impeller into account is visible in Fig. 5. The curves of $d_p^* = f(N \cdot t)$ are more compact than the dependencies $d_p^* = f(t)$ presented in Fig. 4.

Table 1

Model parameters – data Ditl et al. [16]

		N [RPM]	$(P/m)_{imp}$ [W/kg]	k^* [-]	d_{pf} [μm]	R^2 [-]
K1	SQ150-N5000	5 000	4 714	$0.764 \cdot 10^{-5}$	3.816	0.9563
K2	SQ150-N6500	6 500	10 337	$1.476 \cdot 10^{-5}$	3.136	0.9969
K3	SQ150-N7500	7 500	15 867	$1.574 \cdot 10^{-5}$	2.818	0.9882
K4	SQ150-N8800	8 800	25 613	$4.392 \cdot 10^{-5}$	2.500	0.9981
SC1	D300-N3500	3 500	6 440	$1.705 \cdot 10^{-5}$	3.530	0.9955
SC2	D190-N5550	5 550	10 309	$1.549 \cdot 10^{-5}$	3.138	0.9873
SC3	D150-N7600	7 600	16 509	$1.988 \cdot 10^{-5}$	2.790	0.9556
SC4	D100-N11500	11 500	25 485	$1.514 \cdot 10^{-5}$	2.503	0.9278

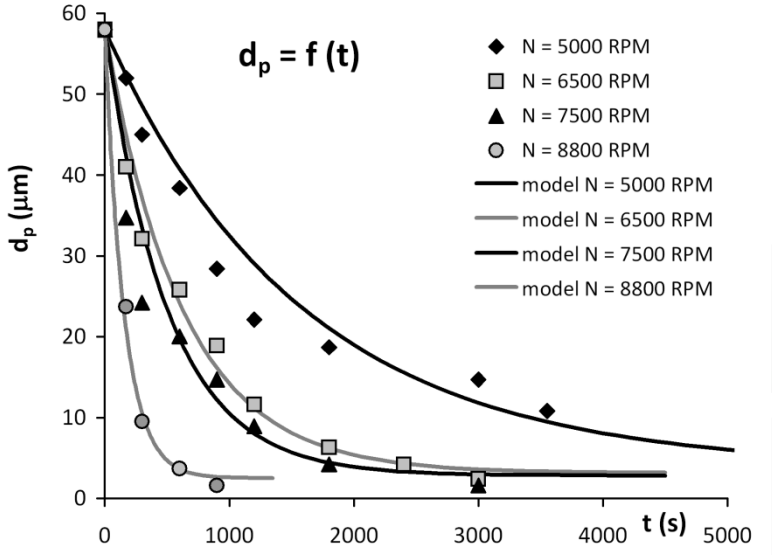

Fig. 1. Experimental data Ditl et al. [16] – squared vessel 150 mm × 150 mm: $d_p = f(t)$

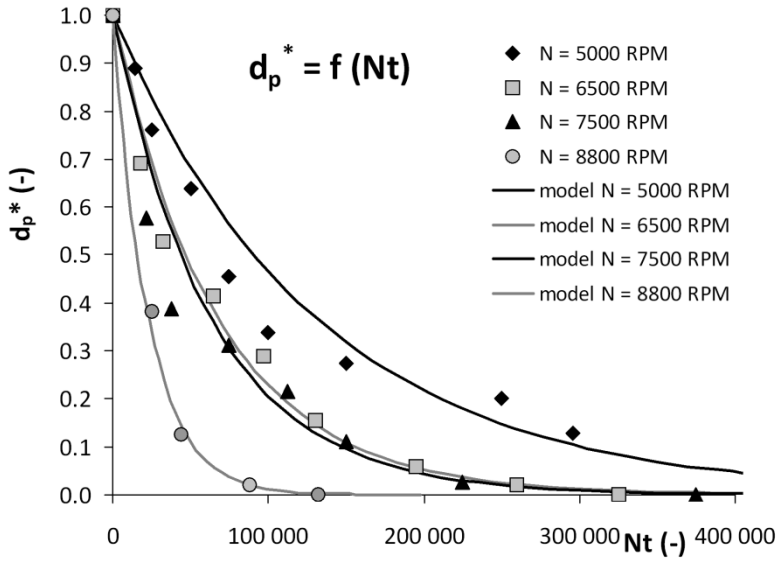

Fig. 2. Experimental data from Ditl et al. [16] – squared vessel 150 mm × 150 mm: $d_p^* = f(N \cdot t)$

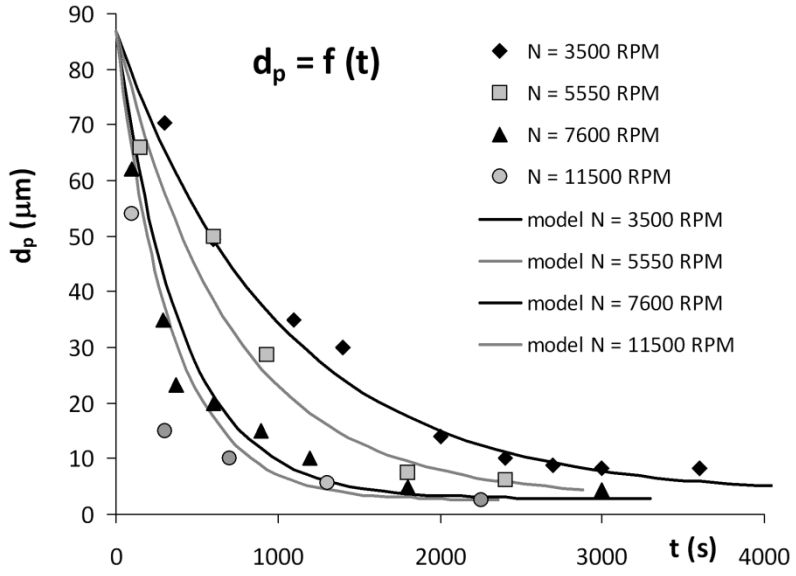

Fig. 3. Experimental data from Ditl et al. [16] – cylindrical vessel scale-up experiment: $d_p = f(t)$

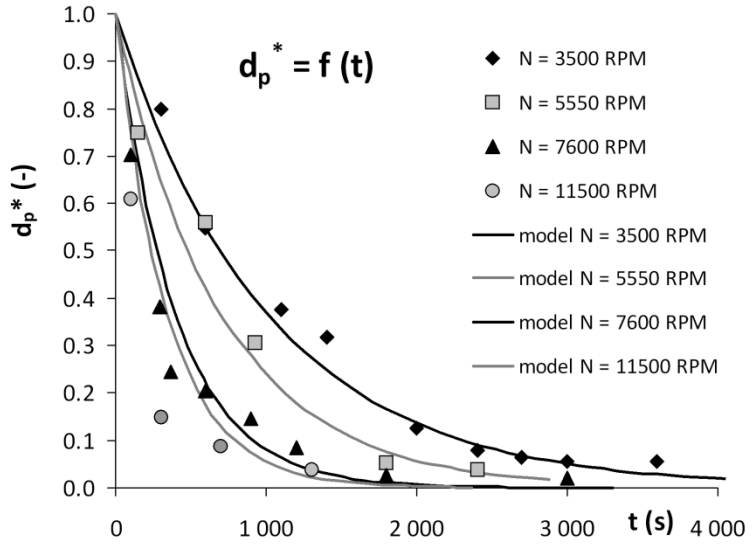

Fig. 4. Experimental data from Ditl et al. [16] – cylindrical vessel scale-up experiment: $d_p^* = f(t)$

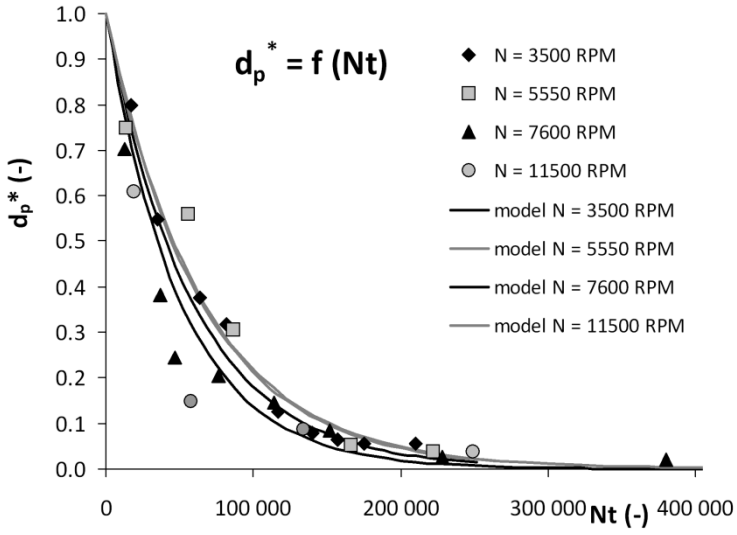

Fig. 5. Experimental data from Ditl et al. [16] – cylindrical vessel scale-up experiment: $d_p^* = f\,(N \cdot t)$

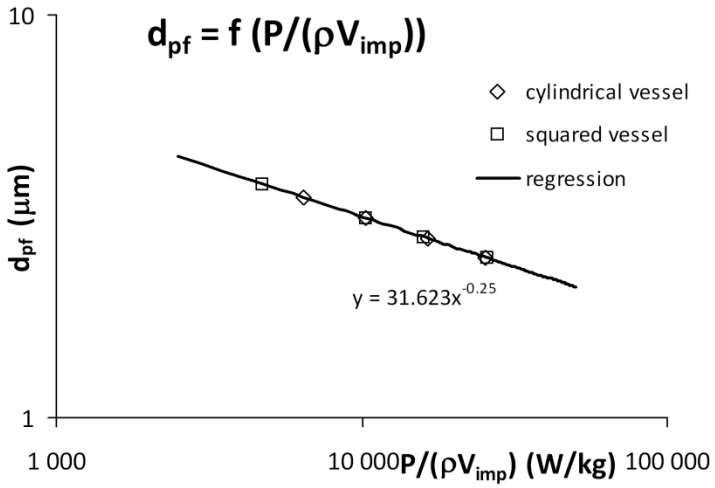

Fig. 6. Experimental data from Ditl et al. [16] – model parameters: $d_{pf} = f\,(P/(\rho \cdot V_{imp}))$; cylindrical vessel – four different vessel sizes, square vessel – four different impeller speeds

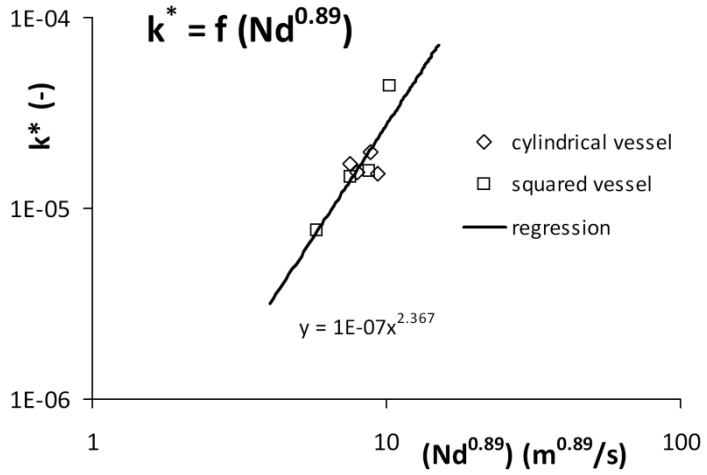

Fig. 7. Experimental data from Ditl et al. [16] – model parameters: $k^* = f\,(N \cdot d^{0.89})$; cylindrical vessel – four different vessel sizes, square vessel – four different impeller speeds

The following dimensional relationships were found for model parameters d_{pf} and k^*:

$$d_{pf} = 31.623 \cdot (P/(\rho \cdot V_{imp}))^{-1/4} \; (R^2 = 1), \tag{10}$$

$$k^* = 1.178 \cdot 10^{-7} \cdot (N \cdot d^{0.89})^{2.367} \; (R^2 = 0.721), \tag{11}$$

where

d_{pf} [μm], k^* [-], $(P/(\rho \cdot V_{imp}))$ [W/kg], N [RPS] and impeller diameter d [m].

As expected, the model parameter d_{pf} is proportional to the mean dissipation rate in the impeller zone $(P/(\rho \cdot V_{imp}))^{-1/4}$ as follows from Equation (9). The dimensionless rate-constant k^* was found to be proportional to shear strength on impeller surface $((N \cdot d)^{0.89})$. The obtained relationships are graphically shown in Fig. 6 and 7.

5. Conclusions

The following conclusions can be made:

A simple dispersion model enabling the prediction of particle size changes over time was proposed. The model takes into account the type of breakup mechanisms, the non-homogeneity of the local turbulent energy dissipation rate in an agitated vessel and the effect of number of times the liquid passes through the impeller and the impeller zone.

The model was successfully tested on the data published by Ditl et al. [16]. In their study, the dispersion of TiO_2 particles in liquid was investigated.

The dimensional relations $d_{pf} = 31.623 \cdot (P/(\rho \cdot V_{imp}))^{-1/4}$ and $k^* = 1.178 \cdot 10^{-7} \cdot (N \cdot d^{0.89})^{2.367}$ were found for model parameters, where d_{pf} [μm], k^* [-], $(P/(\rho \cdot V_{imp}))$ [W/kg], N [RPS] and impeller diameter d [m].

Acknowledgement

This research has been supported by the Grant Agency of the Czech Republic project No. 16-20175S 'Local turbulent energy dissipation rate in dispersion systems.'

References

[1] Paul E.L., Atiemo-Obeng V.A., Kresta S.M. (Eds.), *Handbook of industrial mixing. Science and Practice*, Wiley, Hoboken, NJ, 2004.
[2] Parfitt G.D., *Dispersion of powders in liquids* (2nd ed)., Applied Science Publishers, London 1973.
[3] Lu S., Pugh R.J., Forssberg E., *Interfacial Separation of Particles*, Studies in Interface Science, vol. 20, Elsevier 2005.
[4] Yeoh S.L., Papadakis G., Yianneskis M., *Determination of mixing time and degree of homogeneity in stirred vessels with large eddy simulation*, Chem. Eng. Sci., vol. 60, 2005, 2293-2302.
[5] Cheng D., Feng X., Cheng J., Yang, Ch., *Numerical simulation of macro-mixing in liquid-liquid stirred tanks*, Chem. Eng. Sci., vol. 101, 2013, 272-282.
[6] Sprow F.B., *Distribution of drop sizes in turbulent liquid-liquid dispersions*, Chem. Eng. Sci., vol. 22, 1967, 435-442.
[7] Taylor G.I., *The formation of emulsions in definable fields of flow*, Proc. R. Soc. Lond., A146, 1934, 501-523.
[8] Hinze J.O., *Fundamentals of the hydrodynamic mechanism of splitting in dispersion processes*, AIChE J., vol. 1, 1955, 289-295.
[9] Hu B., Angeli P., Matar O.K., Hewitt G.F., *Prediction of phase inversion in agitated vessels using a two-region model*, Chem. Eng. Sci., vol. 60, 2005, 3487-3495.
[10] Shinnar R., *On the behaviour of liquid dispersions in mixing vessels*, J. of Fluid Mechanics, vol. 10, 1961, 259-275.
[11] Desnoyer C., Masbernat, O., Gourdon, C., *Experimental study of drop size distributions at high phase ratio in liquid-liquid dispersions*, Chem. Eng. Sci., vol. 58, 2003, 1353-1363.
[12] Bałdyga J., Podgórska W., *Drop break-up in intermittent turbulence: maximum stable and transient sizes of drops*, Can. J. of Chem. Eng., vol. 76, 1998, 456-470.
[13] Šulc R., Ditl P., *The effect of process conditions on the flocculation process occurring in an agitated vessel*, Polish J. of Chem. Technology, vol. 14, 2012, 88-96.

[14] Podgórska W., Bałdyga J., *Scale up effects on the drop size distribution of liquid-liquid dispersions in agitated vessels*, Chem.Eng.Sci., vol. 56, 2001, 741-746.
[15] Raikar N.B., Bhatia S.R., Malone M.F., McClements D.J., Almeida-Rivera C., Bongers P., Henson M., *Prediction of emulsion drop size distributions with population balance equation models of multiple drop breakage*, Colloids and Surfaces A: Physicochem. Eng. Aspects, vol. 361, 2010, 96-108.
[16] Ditl P., Novák V., Rieger F., *Dispergace v kapalinách rychloběžnými míchadly (Dispergation in liquids by high-speed impellers)*, Chem.průmysl, vol. 31(56), 1981, 3-10.
[17] Schlichting H., *Boundary layer theory*, McGraw-Hill, New York 1979.